



## EAS Studies of Cosmic Rays with Energy below $10^{16}$ eV

Sunil K. Gupta<sup>1,2;1)</sup>

<sup>1</sup>Tata Institute of Fundamental Research, Homi Bhabha Road, Mumbai 400 005 India

<sup>2</sup>The GRAPES-3 Experiment, Cosmic Ray Laboratory, Raj Bhavan, Ooty 643 001 India

**Abstract:** Here, we summarize the papers involving studies of cosmic rays with extensive air showers below  $10^{16}$  eV that were presented during the 32nd International Cosmic Ray Conference (August 11–18, 2011) in Beijing. A total of 55 papers including oral and poster were submitted. However, 47 papers were actually presented in the conference and only these are discussed. For better organization, we have divided the 47 papers into four broad areas namely, the composition studies, anisotropy studies, other related phenomena, techniques and measurements. A total of 12 papers reported studies of the composition of cosmic rays that included several new results. Many exciting results on the anisotropy of multi-TeV cosmic rays were reported possibly for the first time through nine papers. There were ten papers on various other phenomena that included hadronic properties, search for anti-protons and  $\gamma$ -rays, moon shadow studies etc. A total of 16 papers discussed advances made in various techniques and measurements. The breadth and depth of topics covered in most of the papers was very impressive and the future of the field appears to be really exciting.

**Key words:** extensive air shower, composition, anisotropy, instrumentation

### 1 Introduction

The origin and acceleration of energetic primary cosmic rays continues to remain an outstanding open problem, even after 99 years since their discovery by V.F. Hess in 1912. The extensive air shower (EAS) produced by primary cosmic rays of energy above  $10^{12}$  eV serves as the most effective means for detecting these particles. The 32nd International Cosmic Ray Conference (ICRC) held in Beijing during August 11–18, 2011 witnessed presentation of several exciting new results, specially in the areas of cosmic ray composition and measurement of their anisotropy. Impressive progress was reported on many new measurements of related phenomena with the powerful arrays of detectors currently operating around the world. It is probably safe to state that the field of cosmic ray physics is witnessing a new renaissance on the eve of the centenary of their discovery!

The present work is a summary of the rapporteur talk that was delivered on August 18, 2011, at the

32nd ICRC. It covers the oral and poster presentations in the high energy sessions HE1.1 and HE1.4. In all, a total of 55 presentations were submitted and but only 47 papers were actually presented during the above mentioned sessions that fell within the purview of this talk. While it was not possible to do justice to each presentation, an attempt is made to at least cover most of the highlights in the papers presented. I would like to offer apologies for any mistakes that are yet present, despite my best efforts.

For a better organization, these 47 papers have been broadly classified into four areas, that may be categorized as the composition studies, anisotropy studies, other related phenomena, techniques and measurements. A total of 12 papers reported the studies carried out to probe the spectra and composition of primary cosmic rays. Several new results by the ARGO-YBJ, Tibet AS $\gamma$ , ICECUBE, and BAKSAN experiments were reported at this meeting. Many exciting results on the anisotropy of multi-TeV cosmic rays were also reported for the first time, by

1)E-mail: gupta@grapes.tifr.res.in

the ARGO–YBJ, Tibet AS $\gamma$ , ICECUBE and GRAPES–3 experiments, through a total of nine papers. There were ten reports on various related phenomena that probed hadronic properties, search for antiprotons and  $\gamma$ -rays, the moon shadow studies, the effects of geomagnetic field on EAS etc. A total of 16 papers were devoted to the advances made in various techniques and measurements, and that in itself incorporated a fairly wide spectrum of topics. Undoubtedly, the breadth and the depth of the topics covered in most of the papers was rather impressive, indicating an exciting future ahead for this field. A comprehensive account of earlier EAS studies below  $10^{16}$ eV may be obtained from excellent rapporteur talks delivered in the previous conferences [1–3]. We summarize the composition studies in Section 2. The anisotropy studies are covered in Section 3. Other related phenomena are discussed in Section 4. Various techniques and measurements are presented in Section 5. A brief summary of all papers is given in Section 6 and final section contains acknowledgments.

## 2 Composition studies at energies at and below the “knee” region

ARGO–YBJ is an unconventional EAS array operating at a high altitude of 4300 m above sea level, near Tibet AS $\gamma$  experiment in Yangbajing in Tibet with a full (92%) coverage over an area of nearly 6000 m<sup>2</sup>. It uses resistive plate chambers (RPCs) with excellent time and position resolutions. The capabilities of this array allows real time view of a propagating EAS to be obtained including its structure near the core [4]. By probing the density of particles in an inner and outer region surrounding the core they measured the composition of light components, namely, protons and helium in the energy range from 10 to 300 TeV as shown in Figure 1. Their spectra agrees rather well with direct measurements from CREAM and other experiments [5]. Using a RPC strip multiplicity based trigger the ARGO–YBJ group showed that the data preferentially selects light component (P + He). Although the analysis of data seems to indicate a composition similar to JACEE than CREAM results. However, relatively large error on their data at this stage precluded any definitive conclusions to be drawn [6].

In an innovative approach, two wide-field imaging Cherenkov telescopes, the prototypes for proposed LHAASO (Large High Altitude Air Shower Observatory) experiment were operated alongside ARGO–YBJ. About 0.5 million stereo events from the imag-

ing telescopes were analyzed along with ARGO–YBJ data. With further cuts the combined sample was reduced to 7000 good quality events in the 1–200 TeV energy range. Initial Monte Carlo simulations showed that the relation between ratio of particle densities at 20, 40 m from EAS core and the number of photons detected is sensitive to the composition as seen from Figure 2. The data left of vertical line and above the inclined line were primarily contributed by protons and He nuclei [7].

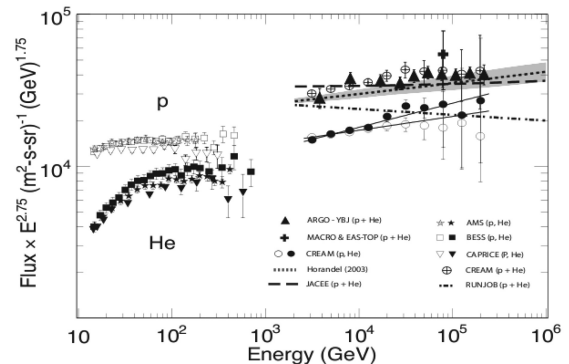


Fig. 1. Unfolding of ARGO–YBJ spectrum by Bayesian approach (QGSJet II + FLUKA + EGS4 + GEANT3).

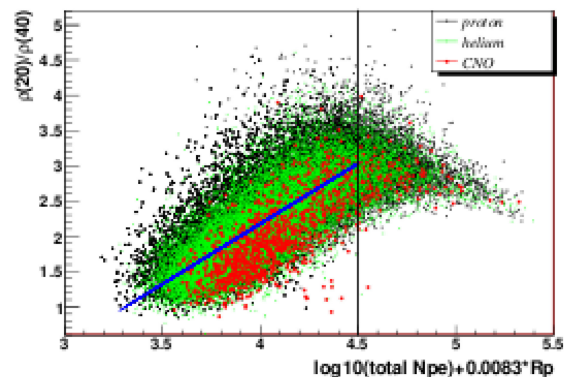


Fig. 2. Dependence of density ratio on total  $N_{pe}$  for p, He, CNO.

Simulation studies were carried out to obtain composition using an artificial neural network (ANN) based on lateral distribution in 30–10000 TeV region for a super ARGO detector 120 m $\times$ 120 m in size. CORSIKA–V.6.90 with QGSJET–II and FLUKA was used to simulate EAS due to p, He, CNO, Fe in five logarithmic energy bins. The simulated data analyzed with cuts on EAS core, direction etc. showed sensitivity to the composition when particle density profile measured in the detector was used. The mean density in 4 m<sup>2</sup> around core was one such parameter [8].

Several results were reported by the Tibet AS $\gamma$  collaboration in association with a suite of new detectors that included Yangbajing air core detectors (YAC-I and II), water Cherenkov muon detectors and so on. Some of these results were extensively covered in the highlight talk on the Tibet AS $\gamma$  experiment [9]. Several parameters including the number of detectors hit, total burst sum, maximum burst size and their various combinations, for a total of eight parameters were used as input to an ANN. Some of these parameters displayed sizable dependence on mass of the primary particle that were exploited to achieve sensitivity to the primary composition. The ANN with 40 hidden nodes was trained by using simulated data [9].

The versatility of their array allowed Tibet AS $\gamma$  to probe hadronic interaction models of cosmic rays at energies above 20 TeV. Preliminary results from analysis using ANN showed that the data agree well with both the QGSJET2 and SIBYLL2.1 models, when non-linear acceleration is assumed. This agreement seems to hold from 30 to 1800 TeV and the results for 260 TeV are shown in Figure 3 [10]. Using the same ANN approach the Tibet AS $\gamma$  collaboration proceeded to separate proton, proton + helium and iron candidate events that were trained for QGSJET2 with a heavy dominated composition. The success of their technique was verified by the ability to extract known contributions of protons, helium and iron nuclei from the Monte Carlo data set. As an example the comparison of assumed and estimated abundances of iron nuclei are shown in Figure 4 and the two agree well within the errors of measurement.

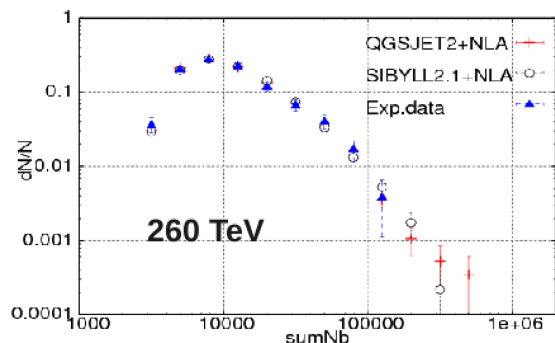


Fig. 3. Dependence of event number on total burst sum.

The fraction of proton, helium and iron nuclei were obtained from an analysis using ANN to obtain the all particle spectrum from Tibet AS $\gamma$  data. This spectrum along with other measurements is shown in Figure 5 [11–13].

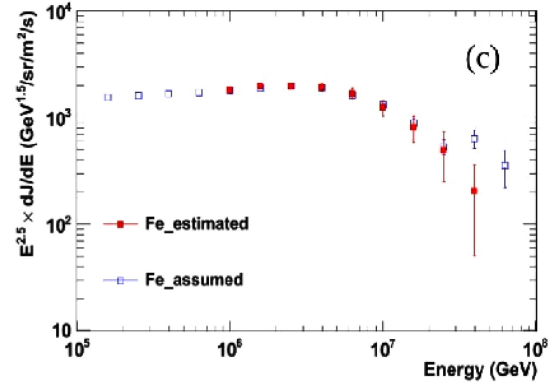


Fig. 4. Assumed and estimated Fe abundances.

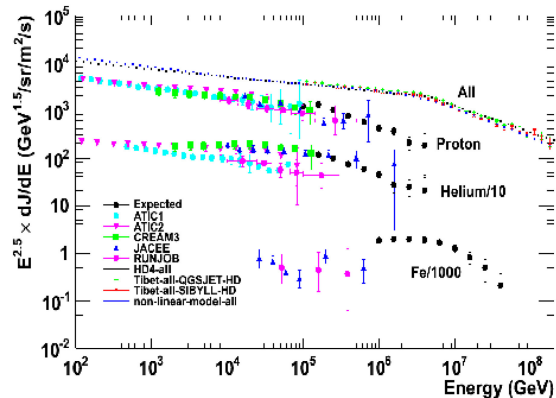


Fig. 5. Tibet AS $\gamma$  all particle energy spectrum.

The ICECUBE collaboration had used muon data collected with 40 strings to extract composition by using the  $N_e$  ( $>1$  MeV from ICETOP) and  $N_\mu$  ( $>500$  GeV) correlation. However, due to limited statistics the composition could be probed only as a combination of protons and iron nuclei. Within the errors of measurements the all particle spectrum was consistent with earlier measurements [14]. In another interesting study the  $\mu$  and  $\nu_\mu$  spectra above 100 GeV were simulated by using primary cosmic ray spectra from KASKADE for five nuclei that were extrapolated with a rigidity dependent “knee” for respective nuclei. The Auger spectra were used at UHE energies and the difference between Auger and extrapolated KASKADE spectra in the overlap energy region was attributed to an extragalactic proton component. These simulations showed that the spectra of both  $\mu$  and  $\nu_\mu$  above 100 GeV were within errors, fully consistent with 40 string ICECUBE measurements. The spectral shape of  $\mu$  and  $\nu_\mu$  appeared to depend only on the all particle spectra and not on the actual composition of primaries. If correct, then this would considerably facilitate accurate calculation of  $\mu$  and  $\nu_\mu$  fluxes at high energies [15].

The BAKSAN had group used high energy muon number spectrum from the BUST detector to study the primary composition in a manner almost independent of the assumed interaction models (QGSJET-I, II, SIBYLL and EPOS). More specifically they showed that the experimental muon number per nucleon varies with the energy per nucleon, independent of interaction model used. The challenge would be to utilize this lack of dependence on the hadronic interaction models to extract the primary composition [16]. The central density ( $N_c$ ) of particles near core in the range  $50\text{--}1.5 \times 10^4 \text{ m}^{-2}$ , and density of muons ( $E_\mu > 1 \text{ GeV}$ ) and hadrons above 30 GeV for each shower was measured by Baksan ‘‘Carpet-2’’ array. From the spectrum of central density the ‘‘knee’’ in the primary spectrum could be seen. The dependence of the ratio  $\langle N_\mu/N_c \rangle$  on energy was claimed to be sensitive to two component composition consisting of protons and iron nuclei. The BAKSAN group plans to use this relation to extract the primary composition in future [17].

### 3 Anisotropy studies at multi-TeV energies

The anisotropy results reported at the Beijing ICRC were undoubtedly one of the outstanding highlights of this event. There were a number of reports from the ARGO-YBJ, Tibet AS $\gamma$ , ICECUBE and GRAPES-3 collaborations that presented detailed structure of the anisotropy in cosmic rays above a few TeV. The early anisotropy measurements date back more than half a century. However, the most satisfying aspect of the current measurements is, that not just the magnitude and the phase of the anisotropy, but even the structure seen in the overlap energy region and fields of view of different experiments are mutually consistent. These measurements also indicate a continuity from the northern to the southern hemisphere in almost a seamless manner. The unprecedented levels of precision achieved in these measurements should allow detailed models of magnetic structures and the flows of multi-TeV cosmic rays to be constructed in the solar neighborhood. These models could then be quantitatively tested against the current observations.

The ARGO-YBJ anisotropy results were comprehensively summarized in a highlight talk [4]. The structure in the anisotropy in the declination band  $10^\circ\text{S}\text{--}70^\circ\text{N}$  was reported as shown in the upper panel of Figure 6. The observed structure showed the presence of both the Loss-cone and Tail-in features, con-

sistent with earlier Tibet AS $\gamma$  results. The data are well described by a sum of two cosine functions as shown in the lower panel of Figure 6. The structure of the anisotropy features showed evolution with energy, where it increased in size and finally broke-up into smaller structures. As shown in Figure 7 even the magnitude of anisotropy varied with energy with a peak at 8 TeV [18]. Using  $2 \times 10^{11}$  events collected over 3 years a medium scale anisotropy ( $5^\circ$ ) at 2 TeV was probed and the presence of two hot spots A and B ( $\sim 0.1\%$ ) first reported by MILAGRO was confirmed. They found a rich structure that showed evidence of evolution in the medium scale features in cosmic ray anisotropy. Several explanations including diffusion from nearby sources, magnetic funneling, and acceleration from magnetic reconnection in solar magnetotail have been proposed to explain these observations [19].

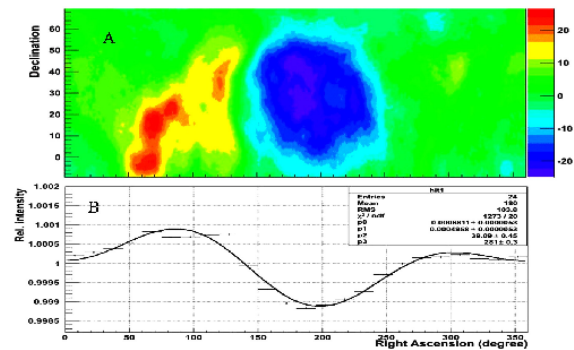


Fig. 6. ARGO-YBJ large scale anisotropy (2008–09).

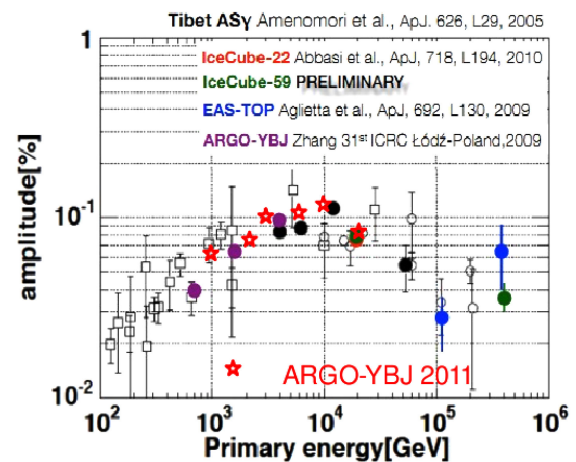


Fig. 7. Energy dependence of ARGO-YBJ anisotropy.

A steadily increasing magnitude of Loss-cone anisotropy was reported by MILAGRO over a period of 7 years (2000–07) at a median energy of 6 TeV. The Tibet AS $\gamma$  group analyzed their data over the same period and examined anisotropy at

three different energies of 4.4, 6.2 and 12 TeV. No evidence of any variability in the magnitude of Loss-cone anisotropy was seen at any of these three energies [20]. The Tibet AS $\gamma$  group had also analyzed data collected over 9 years (1999–2008) to measure the sidereal anisotropy at multi-TeV energies. Sidereal anisotropy at a steady level of 0.1% was observed and it remained nearly unchanged during this period of 9 years, indicating that the TeV cosmic rays were relatively unaffected by the 11-year solar activity occurring during the 23rd cycle [21].

Extensive measurements of large scale anisotropy have made it possible to construct elaborate models to explain the observations. An important effort in this direction attempted to understand the sidereal anisotropy including the Loss-cone and Tail-in features seen by the Tibet AS $\gamma$ . In this model the authors explained observed features as a combination of a global and a mid-scale anisotropy. These anisotropies were attributed to a bi-directional flow along the local interstellar magnetic field and a unidirectional flow of the diamagnetic drift caused by cosmic ray density gradient at multi-TeV energies [22].

New anisotropy results from the southern hemisphere were reported by the ICECUBE collaboration based on muons detected with 59 strings from May 2009 to May 2010. A large statistics allowed anisotropies to be probed at a level of  $10^{-4}$ . As a precursor to these anisotropy studies, the ICECUBE group examined the interference of the solar and sidereal anisotropies. By simulating the solar dipole effects, and the predictions for the integrated effect over an entire year and over a shorter period of three months were compared to the data. The experimental observations for these two different time intervals were found to be in good agreement as shown in Figure 8. As seen from Figure 8, the interference between solar and sidereal anisotropies was well understood within the statistical uncertainties of the data [23]. The results on large scale anisotropy from Tibet AS $\gamma$ , MILAGRO, Super-K and ARGO-YBJ experiments pertain predominantly to the northern hemisphere and the structures reported by these experiments were mutually consistent. However, ICECUBE reported anisotropy from the southern hemisphere for the first time. Thus, in principle, it should be possible to bridge the north-south divide in the cosmic ray anisotropy from these measurements. The seamless variation in Loss-cone and Tail-in anisotropies as seen from Figure 9, from Tibet AS $\gamma$  and ICECUBE at 5 and 20 TeV, respectively, is a testimony to the

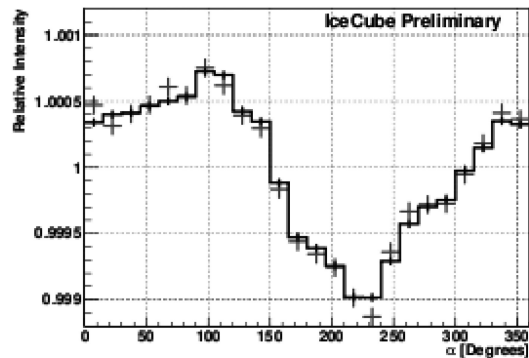


Fig. 8. Crosses represents sidereal anisotropy during 3 months after subtracting the solar anisotropy during this period. The histogram represents sidereal anisotropy over a full year.

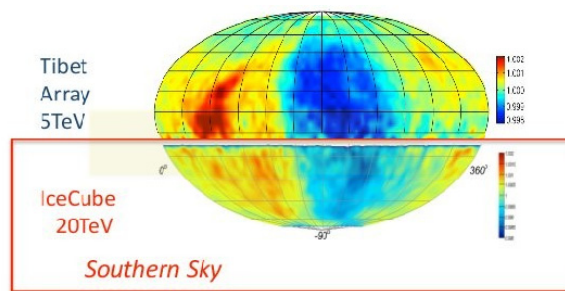


Fig. 9. Loss-cone and Tail-in anisotropies.

power of all sky measurements.

A large muon database was used by ICECUBE to study the anisotropy at three different energies of 20, 400 and 1000 TeV and the results are shown in Figure 10. In a real surprise, the deficit at 20 TeV changed into an excess at 400 TeV and vice-versa. Clearly, better model(s) for the propagation of galactic cosmic rays are needed to explain this unexpected reversal in large scale anisotropy at high energy [24]. The GRAPES-3 collaboration located close to the equator ( $11^\circ\text{N}$ ) reported preliminary anisotropy measurements that span most of the sky except the polar regions and thus, could serve as a bridge between the observatories located in the two hemispheres. The GRAPES-3 results shown in Figure 11 display large scale features consistent with results from other experiments located in both the northern and southern hemispheres [25]. A group from Japan analyzed data collected from two small arrays by using time series of EAS sizes by fractal dimension to select chaotic time series groups. According to authors larger fractal dimension in 5% of groups from 4–7.5 PeV, indicated anisotropy at 5, 11 and 15 h in right ascension [26].

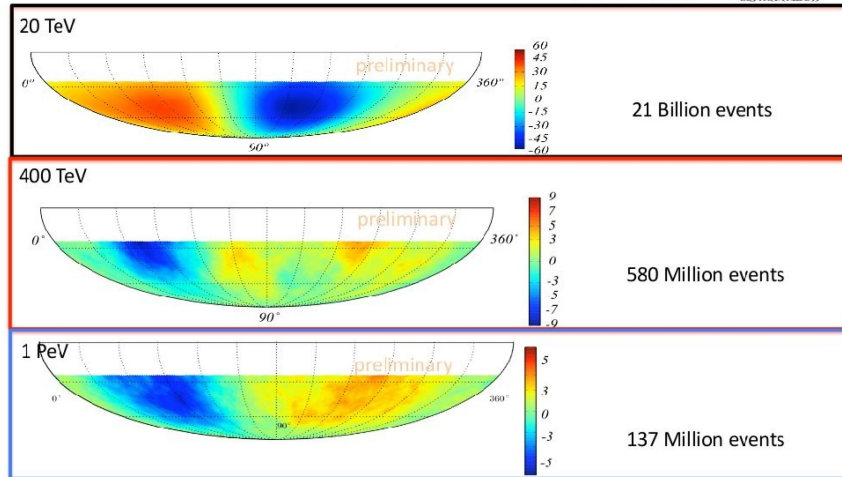


Fig. 10. ICECUBE anisotropy at 20, 400, 1000 TeV.

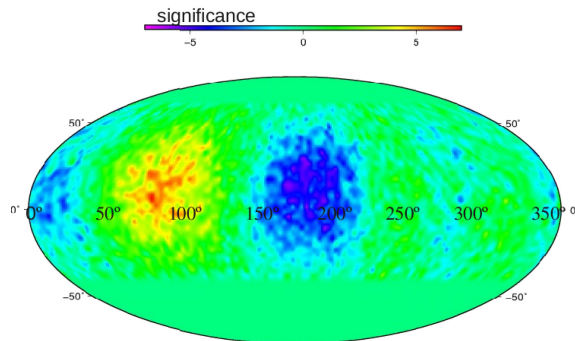


Fig. 11. GRAPES-3 anisotropy at 10 TeV.

#### 4 Studies of other related phenomena

The detection of  $\gamma$ -rays at sub-TeV energies relies on the shape of their Cherenkov images. For EAS ar-

rays the presence of muons, hadrons and EAS front curvature could be used to obtain a better hadron to  $\gamma$  ( $h/\gamma$ ) separation. EAS fronts are characterized by a conical shape and the ARGO-YBJ group, with the aid of simulations showed that this conical factor is much larger for  $\gamma$ -ray than for hadron induced EAS. This was tested by analyzing ARGO-YBJ data on CRAB nebula and the results are shown in Figure 12. Only EAS registering  $>500$  hits were selected. The conical cut enhanced the CRAB signal from  $7.1$  to  $8.4\sigma$  [27]. In another study they used the multi-fractal behavior and lacunarity of secondary particle distributions in EAS front with an ANN to improve the  $h/\gamma$  separation in 1–10 TeV range. Although, actual demonstration of its success with real data is yet to be carried out [28].

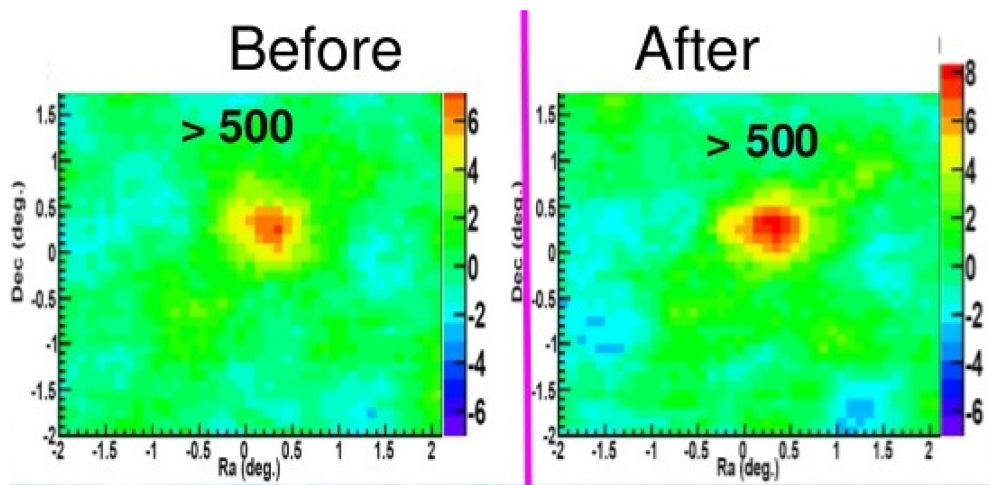


Fig. 12. CRAB image before and after conical cut.

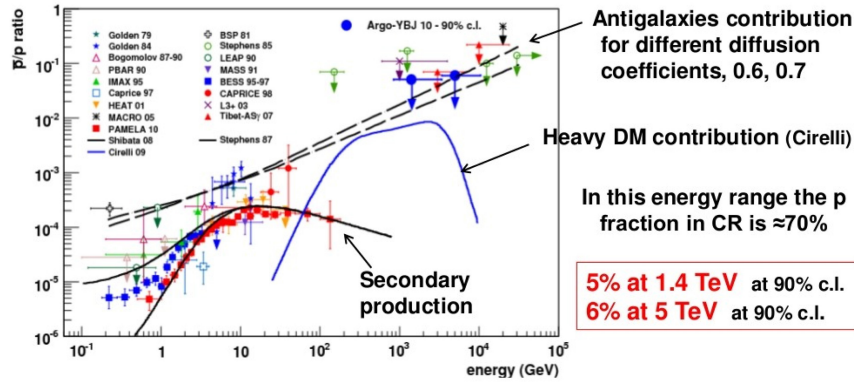


Fig. 13. ARGO-YBJ anti-proton upper limits.

The ARGO-YBJ data was used to detect the shadow of Moon in the cosmic ray sky. At lower energies  $\sim 1$  TeV, the shadow of Moon is shifted west by about  $1.5^\circ$  relative to the actual location of Moon, due to bending of cosmic ray protons in geomagnetic field. The authors had searched for deficit east of Moon location, that could be caused by the presence of anti-protons in cosmic rays. Since no deficit was found, upper limits on anti-proton flux above 1 TeV, competitive with other results were placed, as shown in Figure 13 [29]. In an interesting study the Bose Institute group had simulated production of secondary anti-protons from known primary cosmic ray spectra and a combination of low energy (FLUKA, UrQMD) and high energy (VENUS, QGSJET1, NEXUS, EPOS) hadronic interaction models for the 2001 flight of BESS. As shown in Figure 14, even at relatively low energies (0.2-3 GeV) the BESS anti-proton flux could not be accurately simulated by any of the combinations of models used here [30].

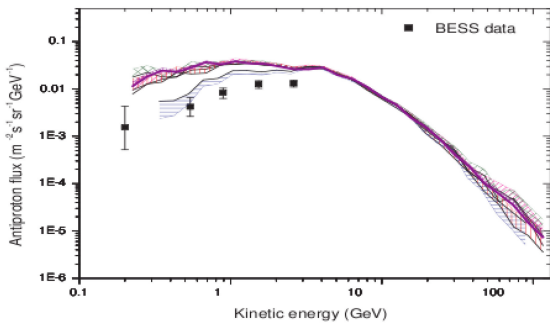


Fig. 14. Simulation results, (a) Horizontally striped band UrQMD1.3 + QGSJET01, (b) vertically striped band FLUKA + QGSJET01, (c) shaded right-tilted band FLUKA + NEXUS, (d) cross-hatched band FLUKA + VENUS, (e) square-hatched band FLUKA + EPOS. Data from BESS-2001 at Ft. Sumner.

The ICECUBE collaboration used  $1.5 \times 10^{11}$  muons collected over four years to measure an annual variation of  $\pm 8\%$  correlated with the atmospheric temperature. This dependence was used to extract the experimental temperature coefficient  $\alpha_T^{\text{exp}}$  from a regression analysis to be  $0.860 \pm 0.002$  (stat.)  $\pm 0.010$  (syst.). The correlation of  $\alpha_T^{\text{exp}}$  and its theoretical counterpart  $\alpha_T^{\text{th}}$  was used to determine the  $K/\pi$  ratio to be  $0.09 \pm 0.04$ . A compilation of the values of  $K/\pi$  ratio is shown in Figure 15 and the ICECUBE value appears to be somewhat lower than other measurements, although

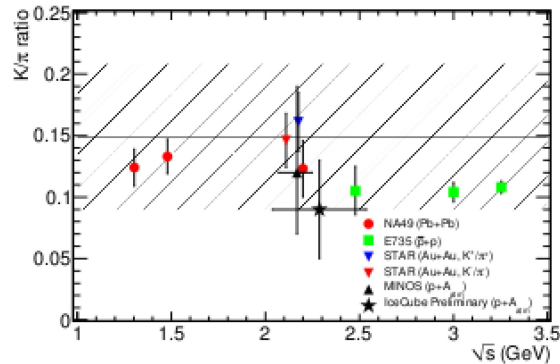


Fig. 15. Compilation of measurements of  $K/\pi$  ratio.

in view of a large error, it may not be considered inconsistent with other measurements [31].

In a fascinating study the ARGO-YBJ group used data collected in 4 1/2 years to measure the displacement of Moon shadow as function of number of triggered strips in their detector to calibrate the energy scale. Using simulations, the relation between strip multiplicity and primary energy was obtained. In Figure 16 the displacement of Moon shadow is shown as a function of hit multiplicity. An excellent agreement is obtained between simulations and data for the rigidity scale from 1.25 to 25 TeV/Z, as labeled at top

of Figure 16 and even a small  $\pm 10\%$  change in scale shown as two dashed curves in Figure 16 result in measurable disagreement with the data [32].

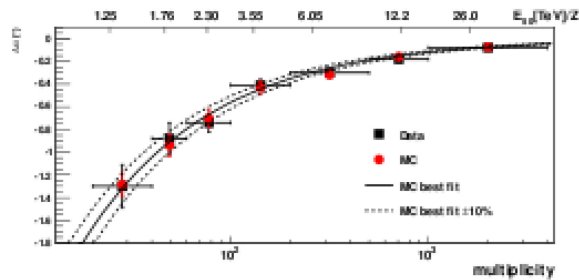


Fig. 16. Solid curve fit to MC and dashed curves represent  $\pm 10\%$  deviation. Energy scale is rigidity (TeV/Z) for the median energy in each multiplicity bin.

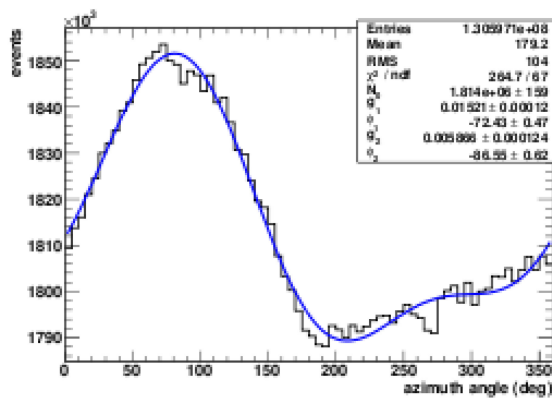


Fig. 17. Azimuthal distribution of ARGON-YBJ events. Smooth curve models effects of geomagnetic field.

A few studies were reported on the effect of geomagnetic field in distorting the lateral distribution of EAS, specially at relatively low energies accessible at high mountain laboratories. The ARGON-YBJ group parametrized the effect of distorted lateral distribution on the azimuthal distribution of particles by a combination of trigonometric functions that included the azimuth of geomagnetic field. A fit to the data with the above function is shown in Figure 17 for azimuthal distribution of events. Clearly, the azimuthal variation ( $\sim 3\%$ ) in Figure 17 is well modeled by the effect of the geomagnetic field [33]. Using a novel approach the North Bengal group carried out simulations using CORSIKA for measuring effect of geomagnetic field on the azimuthal distribution of secondary particles. They showed that separation of charges leads to formation of an effective dipole among muons that was highlighted by introducing the concept of butterfly like regions in opposite quadrants. The muon dipole length as function

of azimuthal direction of the butterfly is shown in Figure 18 for KASKADE and ICETOP experiments for proton and iron primaries that highlights the distortion caused by geomagnetic field. The authors claimed that the muon to electron ratio in different azimuthal sectors carries information on the mass of primary particle [34].

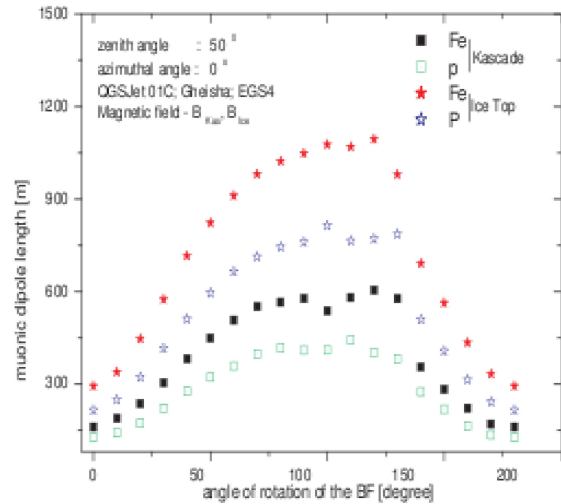


Fig. 18. Variation of muon dipole length with butterfly angle.

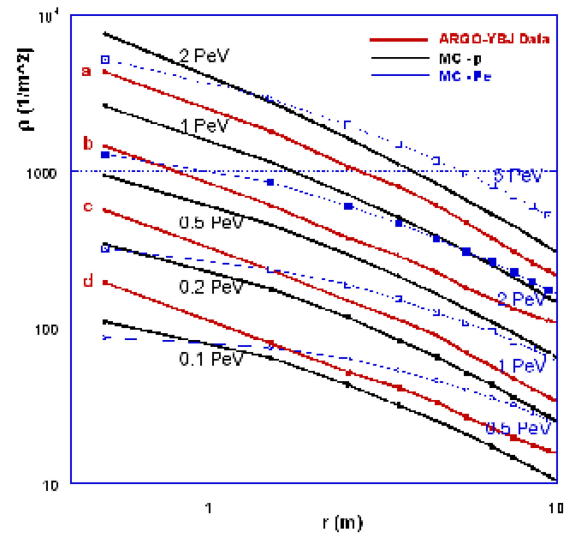


Fig. 19. Lateral distribution near EAS core.

The lateral distribution of EAS above 100 TeV was measured around the shower core in great detail by ARGON-YBJ possibly for the first time. It was done by taking advantage of excellent position and time resolution along with a large dynamic range for particle multiplicity. The observed lateral distribution within 10 m from the core showed significant

departure from the data simulated using proton and iron primaries as shown in Figure 19. These measurements could prove very fruitful in probing the structure of the shower cores [35]. The ICECUBE collaboration had searched PeV  $\gamma$ -rays by analyzing one year of data taken during 2008–09 with 40 strings and 40 surface stations of ICETOP. They derived an upper limit on the ratio of  $\gamma$  to cosmic rays of  $8.1 \times 10^4$  above 1.2 PeV in a region of  $10^\circ$  around the Galactic plane [36].

### 5 Experimental techniques and measurements

Several results were presented, detailing improvements made in a number of experimental techniques and methods of measurements. The PRISMA group reported efforts to develop a detector for measuring thermal neutrons accompanying an EAS to get a handle on its hadronic component. PRISMA is planned to be operated as part of the big LHAASO project. The measured neutron component as function of time is shown in Figure 20. A low number of neutron detected and a long time scale of  $\sim 10$  ms are some of the challenges faced in using this technique for studying hadronic component [37]. For prototype of PRISMA, ZnS(Ag) doped with  $^6\text{Li}$  was found to be an effective scintillator for detecting heavy particles. It produced  $10^5$  photons per neutron capture through a reaction with  $^6\text{Li}$ . Operation of prototype PRISMA around NEVOD–DECOR gave promising results [38]. The NEVOD–DECOR group summarized the status of water Cherenkov detector NEVOD (2000 m<sup>3</sup>), and tracking detector DECOR shown in Figure 21. Investigations of inclined EAS through local muon density spectra can allow exploration of a wide range of energies ( $10^{15}$ – $10^{19}$ eV). This group plans to measure the number and energy of muons in next phase of NEVOD–DECOR [39]. Calibration of TUNKA–133

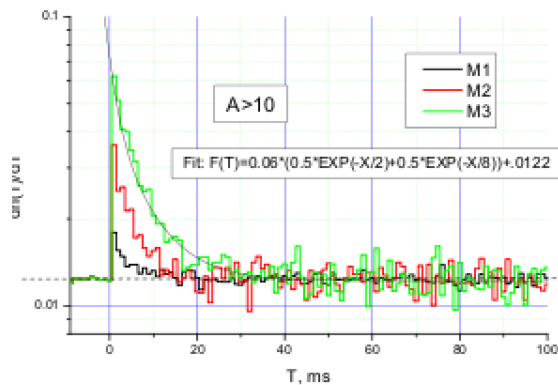


Fig. 20. Time distribution of thermal neutrons.

EAS Cherenkov array used high power InGaN/GaN blue LEDs driven by avalanche transistor drivers, that emit  $\sim 10^{12}$  photons in a pulse of full width at half maximum of 4 ns. The TUNKA–133 collaboration claimed their system to be stable, robust, easy to operate and inexpensive to build [40].

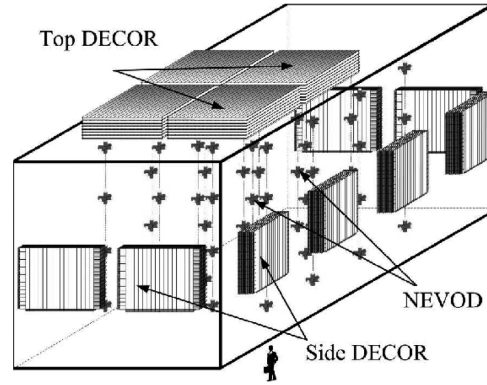


Fig. 21. Schematic of NEVOD–DECOR detector.

LHAASO project KM<sup>2</sup>A, using a 1 km<sup>2</sup> array to be located in Tibet would consist of electron and muon detectors, to probe  $\gamma$ -ray astronomy above 30 TeV and cosmic ray physics in the “knee” region. There were several reports dealing with various aspects of this experiment that are summarized below. Through detailed simulations the LHAASO group determined that primary  $\gamma$ -rays can be identified event by event by using muon content. The observation is background free above 50 TeV with a sensitivity of  $\sim 1\%$  of CRAB, and a high duty cycle of  $>90\%$ . With full-sky survey LHAASO can discover the galactic  $\gamma$ -ray sources and identify cosmic ray sources. Simulations were carried out to optimize detector performance and reach a very high sensitivity as shown in

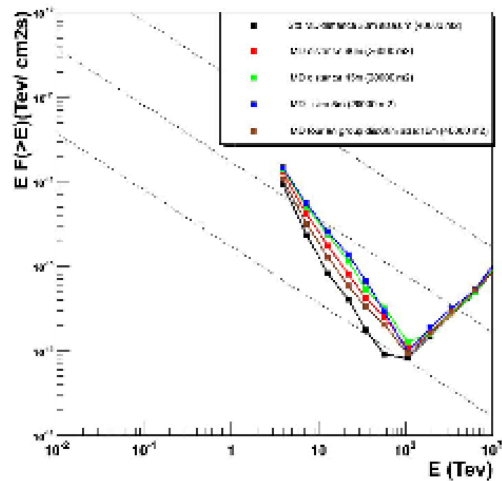


Fig. 22. LHAASO sensitivity for  $\gamma$ -rays.

Figure 22 [41]. Progress on the data acquisition system based on Linux that could meet the exacting requirements of LHAASO was reported [42]. The status of power supplies that could operate with high stability in the extreme weather conditions prevailing at LHAASO site were also reported [43].

The ARGO–YBJ group had exploited the high position and time resolution of their detector to extract the curvature of the shower front that is characterized by a parameter termed conicity. Detailed simulations of EAS and detector response were performed to obtain the correlation between the depth of shower maximum and the conicity parameter as shown in Figure 23. According to the authors the tight correlation seen in Figure 23 offers the hope of exploiting peculiar time structures, like double fronts to probe of the nature of the primary particle [44]. Detailed structure of the EAS near the core region was probed by ARGO–YBJ group using Big pads to extend the dynamic range of particle detection with unprecedented resolution [45]. By using the carpet feature of ARGO–YBJ an excellent time resolution of 200 ps was achieved [46]. By paying special attention to the stability and calibration of analog RPC readout in ARGO–YBJ, its dynamic range could be extended to PeV energies [47]. In another interesting study by employing an iso-gradient method the gains of Big pads were stabilized to better than 1.5% [48]. The effect of  $^{222}\text{Rn}$  daughters on scaler mode of ARGO–YBJ was estimated to be at a level of 1 Hz per  $\text{Bq m}^{-3}$  [49].

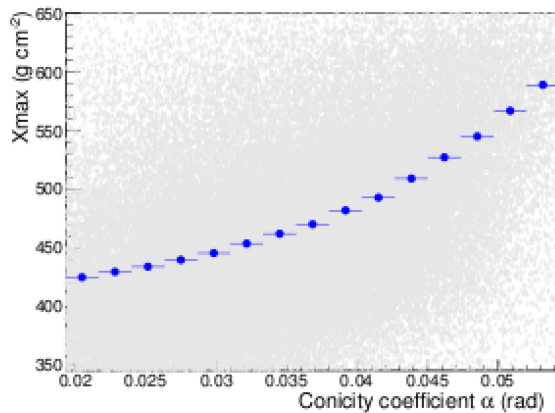


Fig. 23. Depth at shower maximum  $X_{\max}$  from simulations as function of reconstructed conicity  $\alpha$ .

In another report the development of a rugged, stand-alone RPC station for operation in EAS arrays was presented. The RPC station was enclosed in a thermal box made from Al-polyurethane foam, that

was air- and light-tight and was both rigid with good insulation and venting in summer. It required low gas flows and delivered a time resolution of 0.9 ns [50]. In a welcome initiative, there were two reports on public outreach programs. In the first case, two cosmic ray stations consisting of EAS goniometers were being operated in Tbilisi and Telavi in Georgia. Operation in schools, universities etc. are planned in future as part of the GELATICA Network to excite and involve students in cosmic ray research [51]. In the second case as part of public outreach program, the Taipei astronomical museum set up “Cosmic-Gate”, a cosmic ray detector in the summer of 2009. It employed a variety of triggers to demonstrate various cosmic ray effects [52].

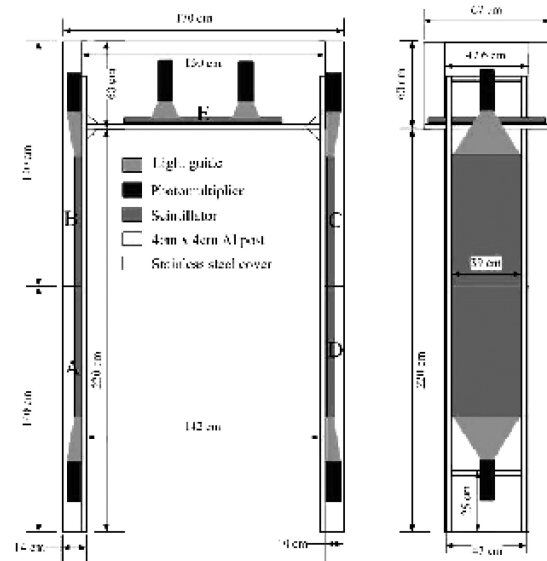


Fig. 24. Cosmic-Gate: A cosmic ray detector for public outreach by Taipei Astronomical Museum.

## 6 Summary

Numerous exciting results were presented on the properties of cosmic rays below and around the “knee” region. With the operation of highly sensitive extensive air shower arrays consisting of a variety of detectors to probe the electromagnetic, muon, hadron and Cherenkov components in an EAS, we are getting progressively better understanding of the composition and energy spectrum in the “knee” region. The operation of proposed new experiments, specially LHAASO may well address this longstanding problem with much higher sensitivity. The highlight of the 32nd ICRC undoubtedly were the multi-TeV anisotropy measurements reported by the ARGO–YBJ, ICECUBE, Tibet AS $\gamma$  and GRAPES–3 experi-

ments that have provided a consistent picture across the two hemispheres. These measurements pose interesting questions that need to be answered through new and innovative models of cosmic ray propagation, specially in the solar neighborhood. There were several other reports on related phenomena that suggest an exciting future ahead of us. The continuing developments in experimental techniques and measurements bode well for the improvement in the sensitivity of existing and proposed experiments. Therefore, on the eve of the centenary of the discovery of cosmic rays by V.F. Hess in 1912, the future of the field appears to be brighter than ever before.

## 7 Acknowledgments

I am grateful to the organizers of the 32nd International Cosmic Ray Conference in Beijing for providing

this wonderful opportunity to summarize the work of so many distinguished colleagues. Special thanks are due to Hongbo Hu and his colleagues for warm hospitality during my stay in Beijing and for providing every possible help during the preparation of this manuscript. I am grateful to a number of colleagues for numerous discussions including, Narayana Bhat, Shashi Dugad, Ralph Engel, Jordan Goodman, Andreas Haungs, Yoshio Hayashi, Hongbo Hu, Johannes Knapp, Paolo Lipari, Sibaji Raha, Subir Sarkar and several others. I specially thank the authors of the oral and poster presentations covered here, for patiently explaining their work that greatly assisted the preparation of this manuscript. I would like to place on record my deep appreciation of colleagues both at Ooty and Mumbai for their assistance and interaction, in addition to their continuous and tireless contributions to the GRAPES-3 program.

## References

- [1] J. Mathews, 2005, ICRC, 10, 283
- [2] R. Engel, 2007, ICRC, 6, 359
- [3] H. Hu, 2009, ICRC (rapporteur), arXiv:0911.3034
- [4] B. D’Ettorre Piazzoli, 2011, ICRC (highlight), in press
- [5] S. M. Mari and P. Montini, 2011, ICRC, 1, 22
- [6] B. Panico and G. Di Sciascio, 2011, ICRC, 1, 26
- [7] S. Zhang, 2011, ICRC, 1, 42
- [8] A. Cirillo and S. M. Mari, 2011, ICRC, 1, 82
- [9] J. Huang, 2011, ICRC (highlight), in press
- [10] J. Shao, 2011, ICRC, 1, 149
- [11] J. Huang, 2011, ICRC, 1, 153
- [12] D. Chen, 2011, ICRC, 3, 297
- [13] Y. Zhang, 2011, ICRC, 1, 157
- [14] K. Rawlins, 2011, ICRC, 1, 101
- [15] D. Bindig, 2011, ICRC, 1, 161
- [16] V. B. Petkov, 2011, ICRC, 1, 10
- [17] D. D. Dzhappuev, 2011, ICRC, 1, 94
- [18] S. Cui, 2011, ICRC, 1, 6
- [19] G. Di Sciascio, 2011, ICRC, 1, 74
- [20] T. Saito, 2011, ICRC, 1, 62
- [21] Y. Zhang, 2011, ICRC, 1, 137
- [22] T. Sako, 2011, ICRC, 11, 105
- [23] R. Abbasi, 2011, ICRC, 1, 58
- [24] R. Abbasi, 2011, ICRC, 1, 54
- [25] A. Oshima, 2011, ICRC, 1, 109
- [26] S. Ohara, 2011, ICRC, 1, 70
- [27] X. Li, 2011, ICRC, 1, 46
- [28] A. Pagliaro, G. D’Alistaiti and F. D’Anna, 2011, ICRC, 1, 125
- [29] G. Di Sciascio, 2011, ICRC, 1, 30
- [30] R. Sibaji, 2011, ICRC, 1, 129
- [31] P. Desiati, 2011, ICRC, 1, 78
- [32] G. Di Sciascio and R. Iuppa, 2011, ICRC, 1, 34
- [33] P. Bernardini, et al., 2011, ICRC, 1, 86
- [34] J. N. Capdevielle, 2011, ICRC, 1, 133
- [35] M. Iacovacci, 2011, ICRC, 1, 113
- [36] S. Buitink, 2011, ICRC, 1, 105
- [37] Y. V. Stenkin, 2011, ICRC, 3, 21
- [38] Y. V. Stenkin, 2011, ICRC, 3, 259
- [39] I. I. Yashin, 2011, ICRC, 3, 76
- [40] B. K. Lubsandorzhev, 2011, ICRC, 3, 239
- [41] X. Ma, 2011, ICRC, 3, 157
- [42] M. Gu, 2011, ICRC, 3, 255
- [43] X. Sheng and S. Zhang, 2011, ICRC, 3, 274
- [44] G. Marsella, 2011, ICRC, 1, 66
- [45] M. Zha, 2011, ICRC, 1, 38
- [46] S. Mastroianni, 2011, ICRC, 3, 227
- [47] M. Iacovacci and S. Mastroianni, 2011, ICRC, 1, 117
- [48] X. Ma, 2011, ICRC, 1, 90
- [49] E. Giroletti, 2011, ICRC, 1, 18
- [50] M. Pimenta, 2011, ICRC, 3, 129
- [51] M. Svanidze and Y. Verbetsky, 2011, ICRC, 3, 2
- [52] M. A. Huang, 2011, ICRC, 3, 164